

Polycarbonate nanoplastics and the *in vitro* assessment of their toxicological impact on liver functionality

Valentina Tolardo^{1,2,#}, *Alessio Romaldini*^{3,#}, *Francesco Fumagalli*⁴, *Andrea Armirotti*⁵, *Marina Veronesi*^{6,7}, *Davide Magri*^{4,†}, *Stefania Sabella*^{3,*}, *Athanassia Athanassiou*¹, *Despina Fragouli*^{1,*}

¹Smart Materials, Istituto Italiano di Tecnologia, Via Morego, 30, 16163 Genova, Italy

²Department of Informatics, Bioengineering, Robotics and Systems Engineering, University of Genova, Via All'Opera Pia, 13, 16145 Genova, Italy

³Nanoregulatory Group, D3 PharmaChemistry, Istituto Italiano di Tecnologia, Via Morego, 30, 16163 Genova, Italy

⁴European Commission, Joint Research Centre (JRC), Ispra, Italy

⁵Analytical Chemistry Laboratory, Istituto Italiano di Tecnologia, Via Morego, 30, 16163 Genova, Italy

⁶D3-PharmaChemistry, Istituto Italiano di Tecnologia, Via Morego 30, 16163 Genova, Italy

⁷Structural Biophysics and Translational Pharmacology, Istituto Italiano di Tecnologia, Via Morego 30, 16163 Genova, Italy

*Author for correspondence: stefania.sabella@iit.it, despina.fragouli@iit.it

#These authors contributed equally

†Current address: GenScript Biotech, B.V. Treubstraat 1, 2288EG, Rijswijk, Netherlands

Supplementary information on Materials and Methods

S1. Evaluation of the particles concentration

To evaluate the amount of the PC particles produced, in terms of mg/mL, the weight of ablated product in a stock sample was quantified by means of thermogravimetric analysis (TGA) (Q500, TA Instruments-Waters Spa, Milano, IT). Measurements were performed adding 80 μ L of the particles dispersion in a platinum pan, and an isotherm was recorded at 100°C until the stabilization of the pans weight to a constant value, in order to permit to the water to evaporate under inert N₂ atmosphere (N₂ flow rate: 50 mL/min). In this way, the concentration of the specific dispersion was defined. Subsequently, the UV-vis spectra of that dispersion, as well as of other dispersions after the appropriate dilution, were recorded using a Varian CARY 6000i UV-Vis spectrophotometer (Walnut Creek, CA, USA) in order to construct a calibration curve by plotting the absorbance at the wavelength of 278 nm for each concentration.

S2. Evaluation of the colloidal stability

The colloidal stability of the PC-NPs in complete HHPM (*i.e.*, fully supplemented Hepatocyte High Performance Medium; Upcyte Technologies GmbH, Hamburg, DE) was evaluated as a function of the incubation time (up to 48 hours) by DLS analysis. The PC-NPs dispersion was diluted at 30 μ g/mL in complete HHPM and incubated directly in the cuvette for DLS measurements at 37°C for 0, 24, and 48 hours. To study the surface charge of particle-corona complexes derived from the incubation in complete HHPM, each dispersion, at the end of the incubation time, was centrifuged at 20000g for 15 minutes at 4°C, and the corresponding pellet was washed three times with a volume of Milli-Q® water equal to the initial volume of the dispersion^{1,2}. The surface charge of particle-corona complexes was

measured via Z-pot analysis and compared to the bare PC-NPs (*i.e.*, particles not incubated in complete HHPM). Three consecutive measurements were run for all the samples.

S3. Raman and X-ray photoelectron spectroscopy (XPS) studies

Chemical characterization was performed with Raman analysis (LabRam HR800, Horiba Jobin-Yvon Inc., France). The spectrometer was equipped with a built in microscope with the 632.8 nm He-Ne laser excitation. Post-ablated and concentrated (by Rotavapor treatment) PC-NPs mixtures were drop casted on a silicon substrate and dried at RT. A pristine PC film (4 mm²) was also analyzed after being washed with ethanol followed by Milli-Q[®] water for its purification. The spectra were recorded in the spectral range from 360 to 3600 cm⁻¹ and with a 100x objective lens with a spectral resolution of approximately 1 cm⁻¹. For the pristine PC, for each spectrum the acquisition time was 180 s, and the final spectrum was a result of 20 repetitions, while for the PC-NPs dispersion the acquisition time was 20 s with 10 accumulations. Graphical representation and normalization were performed with Origin Pro version of 2018 v9.5 software.

The surface chemistry was evaluated by X-ray photoelectron spectroscopy (XPS) using an Axis Ultra spectrometer (Kratos Analytical) with Al K α source ($h\nu = 1486.6$ eV) operated at 15 kV with an emission current of 10 mA and a x-ray spot size of 100×100 μm^2 . The residual pressure of the analysis chamber was less than 8×10^{-9} Torr. For each sample, both survey spectra (0 –1150 eV, pass energy 80 eV) and high-resolution spectra (pass energy at 40 eV) were recorded. Charge neutralizer consisting of low-energy electrons was applied and energy scale calibration was performed by setting the C-C/C-H component of C1s spectrum at 285.0 eV. NPs films were prepared by drop/casting using Teflon strips as substrates. Teflon substrates allow minimizing the uncertainties in the stoichiometric evaluation of the C content of the surface, mainly due to adventitious hydrocarbon contamination. This is especially critical in case of low thicknesses of the analyzed films, as the high binding energy shift of electrons originating

from C-F bonds and the precisely known Teflon stoichiometry allows separating with high confidence the substrate and sample contributions during the C 1s peak fitting. Accordingly, Teflon substrate contribution to the C 1s signal was not considered in the elemental quantification of the sample. Sample preparation procedures established in literature were followed for solid ³ and nanoparticles ⁴ surfaces, respectively. Spectra were processed using Vision2 software (Kratos Analytical, UK), and the analysis of the XPS peaks was carried out using a commercial software package (CasaXPS v2.3.18PR1, Casa Software, Ltd., UK). Peak fitting was performed with no preliminary smoothing. Symmetric Gaussian–Lorentzian (70% Gaussian and 30% Lorentzian) product functions were used to approximate the line shapes of the fitting components after a 3-parameters Tougaard-type background subtraction.

S4. ¹H Nuclear Magnetic Resonance (NMR) analysis

The molecular components of the dispersant were analyzed by NMR spectroscopy. All NMR experiments were recorded at 25°C with a Bruker FT NMR AvanceIII and AvanceNeo 600 MHz spectrometer (Bruker Corporation, Billerica, MA, USA) equipped with a 5-mm CryoProbe QCI ¹H/¹⁹F-¹³C/¹⁵N-D-Z quadruple resonance with shielded z-gradient coil, and the automatic sample changer SampleJet™ with temperature control. For all samples a ¹D ¹H spectrum with water suppression was obtained using the standard NOESY (nuclear Overhauser effect spectroscopy) presat Bruker pulse sequence, with 64 k data points, a spectral width of 30 ppm, 128 scans, an acquisition time of 1.84 s, a relaxation delay (d1) of 4 s and a mixing time of 100 μs. In each 5mm NMR tube were added 450 μL of sample plus 50 μL of D₂O (for the lock signal) and 200 μM of 3-propionic-2,2,3,3-d₄ acid (TSP, for the ¹H chemical shift reference). To verify the presence of BPA, we added BPA in the dispersant, at a final concentration of 2mM and we recorded the NMR spectrum. Spectra before and after the BPA addition were compared in order to identify the BPA peaks.

S5. Liquid Chromatography – Mass Spectrometry (LC-MS) analysis

The molecular components of the dispersant were also analyzed by high-resolution mass spectrometry, without any further purification as described in the Supporting Information Section S2. Data were acquired in positive (ESI+) and negative (ESI-) ion modes with an ACQUITY UPLC system coupled to a Synapt G2 QToF high-resolution mass spectrometer (Waters, Milford, MA, USA). The column used to separate the molecular components was an ACQUITY UPLC® HSS T3, 1.8 μm internal diameter, 2.1x50.0 mm (Waters). Eluents were water with formic acid 0.1% v/v (A) and acetonitrile with formic acid 0.1% v/v (B) (Aldrich, Milano, IT). Injection volume was 3 μL for ESI+ and 5 μL for ESI-, and the flow rate 0.450 mL/min. The column was kept at 45°C. Samples were eluted with a linear gradient of eluent B in A for 5 minutes before reconditioning. The total run time was 8 minutes. The scan range was set from 50 to 600 m/z (sensitivity mode). Cone voltage was 30 V, the source temperature was set to 90 °C, desolvation gas flow was 700 L/h and the cone gas flow was 20 L/h for both ESI+ and ESI-, while the desolvation temperature was set to 400 °C. Data were acquired in MSE mode, alternating MS and MS/MS scans. The scan time was 0.3 s, and the low collision energy was set to 4 eV. The real-time spectra recalibration was done using leucine enkephalin (2 ng/mL) as lock mass. From the total extract chromatograms, the most intense m/z values were manually analyzed with MassLynx (Waters Inc., Milford, MA, USA) and annotated for both ESI+ and ESI- polarities following already available references ⁵.

S6. Cell viability assay

Resazurin reduction test was used for determining the cell viability after treatment with PC-NPs dispersions. At P3, UHHs were seeded into collagen-coated flat bottom 96-well plates (growth area: $\sim 0.3 \text{ cm}^2$; $\sim 1.2\text{E}5 \text{ cells/cm}^2$) and, the day after, were treated with increasing concentrations of PC-NPs (0.1 mL/96-well) for 24 or 48 hours. Cells treated with complete medium supplemented with 0.03% Triton X-100 (Sigma Aldrich-Merck KGaA, Darmstadt, DE) for 24 or 48 hours were used as a positive

control of cell viability reduction. At the end of any time interval, stimulation media were replaced with 44 μ M resazurin sodium salt (Sigma Aldrich-Merck KGaA, Darmstadt, DE) in serum-free phenol red-free high glucose DMEM (Sigma Aldrich-Merck KGaA, Darmstadt, DE) and, after 1 hour of incubation, resazurin solution was transferred into a clean 96-well plate. Fluorescence was read at 535 nm by Tecan Spark[®] reader (Tecan, Männedorf, CH). Three independent experiments were carried out, each arranged with a technical triplicate. In each experiment, a couple of cell-free collagen-coated wells per stimulation condition was incubated under the same conditions and used as the blank value for removing potential interferences. Results are reported as percentages (means \pm SD) of the control (set as 100%).

S7: Cytotoxicity assay

CytoTox96[®] Non-Radioactive Cytotoxicity Assay (Promega Corporation, Madison, WI, USA) was used for evaluating the cell membrane integrity after the treatment with PC-NPs dispersions. At the end of any incubation time interval, stimulation media derived from the cell viability assay were saved, centrifuged at 20000g for 15 minutes at 4°C and analyzed following the manufacturer's instructions. The condition "0.03% Triton X-100" was used as positive control of cell membrane damage. Three independent experiments were carried out, each arranged with a technical triplicate. In each experiment, a couple of cell-free collagen-coated wells per stimulation condition was incubated under the same conditions and used as the blank value for removing potential interferences. Results are reported as percentages (means \pm SD) of the positive control (set as 100%).

S8: Reverse transcription and quantitative Real-Time PCR

At P3, UHHs were seeded into collagen-coated flat bottom 24-well plates (growth area: \sim 2.0 cm²; \sim 9.5E4 cells/cm²) and treated at the confluence with increasing concentrations of PC-NPs dispersions (0.667 mL/24-well) for 24 or 48 hours. Using the same experimental setting, confluent cells were also

treated with the isolated PC-NPs, the dispersant, or the filtered water, as described above. At the end of each time interval, cells were extensively washed with DPBS (Sigma Aldrich-Merck KGaA, Darmstadt, DE) and incubated at -80°C with TRIzol™ Reagent (0.5 mL/24-well; Invitrogen-Thermo Fisher Scientific, Waltham, MA, USA). Total RNA was isolated following Chomczynski's protocol ⁶ and reverse-transcribed to first-strand cDNA (2 µg of RNA per sample in a 20-µL reaction) using SuperScript™ VILO™ cDNA Synthesis Kit (Invitrogen-Thermo Fisher Scientific, Waltham, MA, USA) following the manufacturer's instructions. For each target gene, the transcript level was measured via quantitative Real-Time PCR (qPCR), using iTaq™ Universal SYBR® Green Supermix (Bio-Rad, Hercules, CA, USA) on Applied Biosystems ViiA 7 Real-Time PCR System (Life Technologies-Thermo Fisher Scientific, Waltham, MA, USA). Nucleotide sequence, temperature of annealing, qPCR efficiency and amplicon size of each primer pair are reported in Romaldini et al. ⁷. The *gapdh* gene was used as reference gene. For each primer pair, primer specificity was confirmed by melting curve analysis. The quantification of each target transcript relative to the control condition was calculated using Pfaffl's model ⁸. Results are means ± SD of three independent experiments.

S9: Western blot

In parallel with gene expression analysis, protein content analysis was performed via western blot. Starting from the same homogenates used for RNA isolation, total proteins were isolated following Chomczynski's protocol ⁶ and quantified using Pierce™ BCA Protein Assay Kit (Thermo Scientific™-Thermo Fisher Scientific, Waltham, MA, USA), as indicated by the manufacturer. Total proteins (10 µg/sample) were run on NuPAGE™ 4-12% Bis-Tris gel (Invitrogen-Thermo Fisher Scientific, Waltham, MA, USA) under reducing conditions, and transferred to Amersham™ Protran™ 0.2 µm NC nitrocellulose blotting membrane (GE Healthcare, Buckinghamshire, UK). The membrane blocking, the procedure of antibody incubation, the protein detection and the densitometric analysis were carried out

as previously reported ⁷. Antibodies raised against CYP3A4 (1:1000; Cell Signaling Technology, Danvers, MA, USA) and albumin (1:1000; Cell Signaling Technology, Danvers, MA, USA) were used for detecting target proteins while anti-GAPDH antibody (1:1000; Abcam, Cambridge, UK) was used for detecting the internal control. Results, reported as n-fold increase over the control conditions, are means \pm SD of three independent experiments.

S10. CYP2C9 activity assay

At P3, UHHs were seeded into collagen-coated, flat-bottom 96-well plates (growth area: \sim 0.3 cm²; \sim 8.5E4 cells/cm²) and treated at the confluence with increasing concentrations of PC-NPs (0.1 mL/96-well) for 24 or 48 hours. At the end of each time interval, cells were manipulated as described in Romaldini et al. ⁷. Three independent experiments were carried out, each arranged with a technical triplicate. In each experiment, a couple of cell-free, collagen-coated wells per stimulation condition was incubated under the same conditions, manipulated as done with cells, and used as the blank value for removing potential interferences. Results are reported as percentages (means \pm SD) of the control (set as 100%).

S9S11. Statistical analysis

Statistical analysis was run on Prism (GraphPad Software, San Diego, CA, USA). Ordinary one-way ANOVA was used for analyzing data from cell viability assay, cytotoxicity assay, qPCR analysis, western blot analysis, and CYP2C9 activity assay. If ANOVA revealed significant differences within a data set, Dunnett's multiple comparisons test was used. Differences were considered statistically significant as the p-value was lower than 0.05. All reported data are means \pm standard deviations (SD) of three independent experiments.

Supplementary Figures

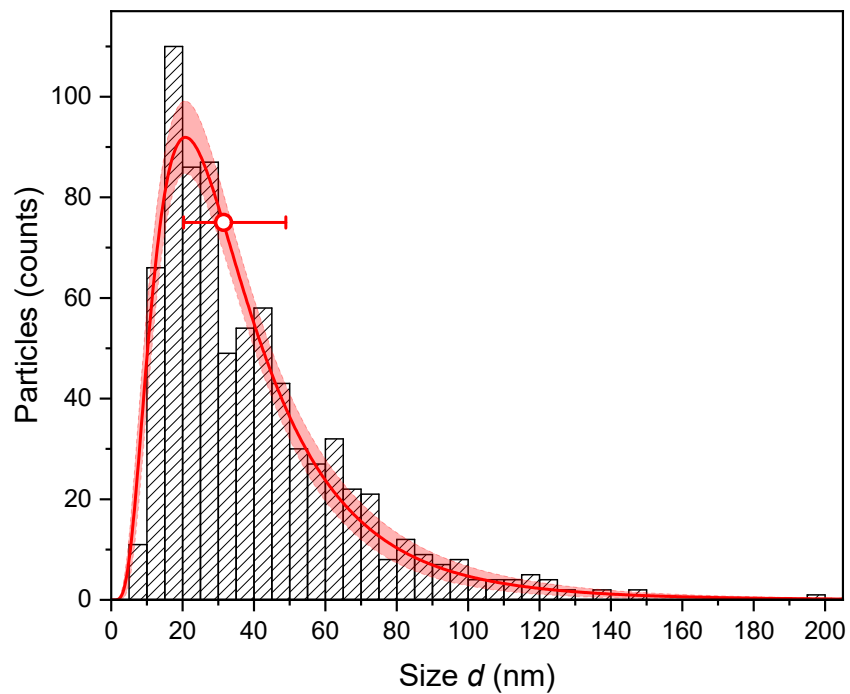


Figure S1. Lateral size distribution of PC-NPs calculated using different TEM images (mean size equal to 31.5 nm; scatter intervals = -20.3, + 48.9 nm).

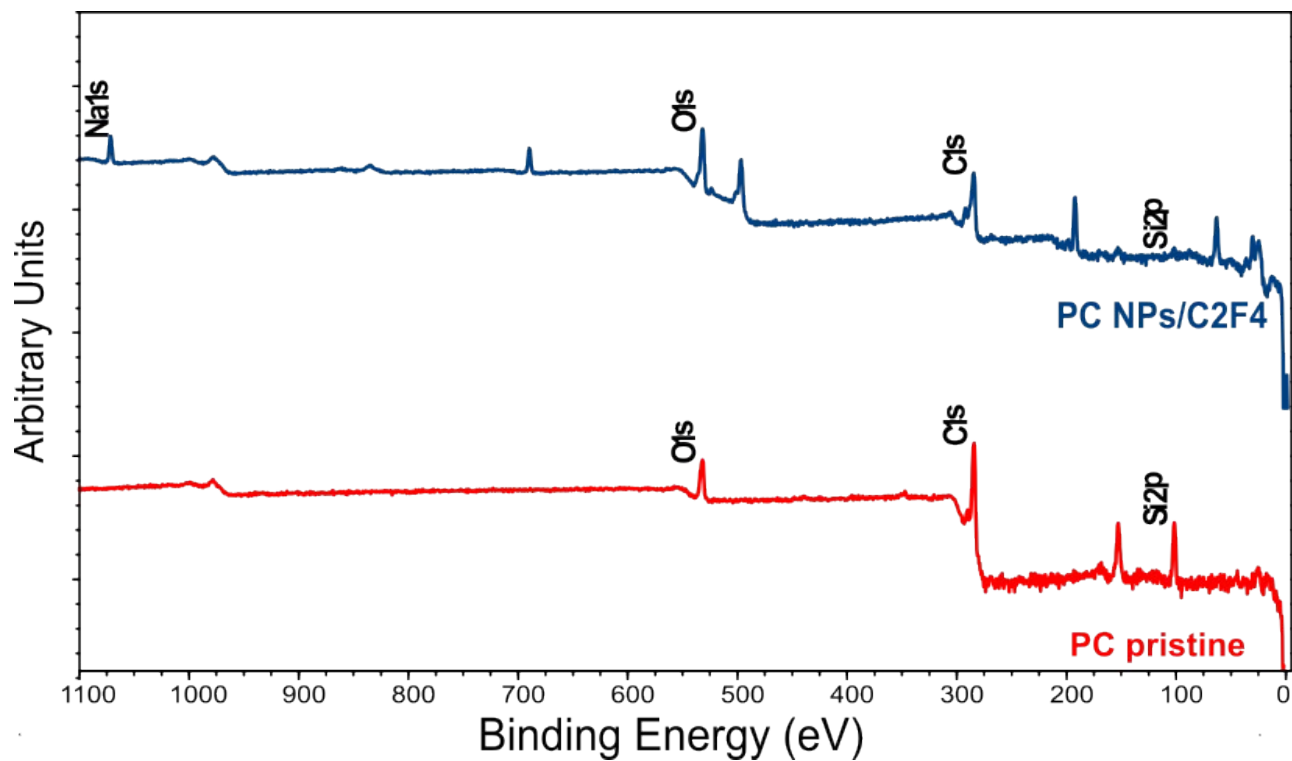


Figure S2. Survey XPS spectra of the pristine polymer and of the as-synthesized NPs with the respective elemental composition. NP dispersion drop-casted on Teflon (C₂F₄) substrate.

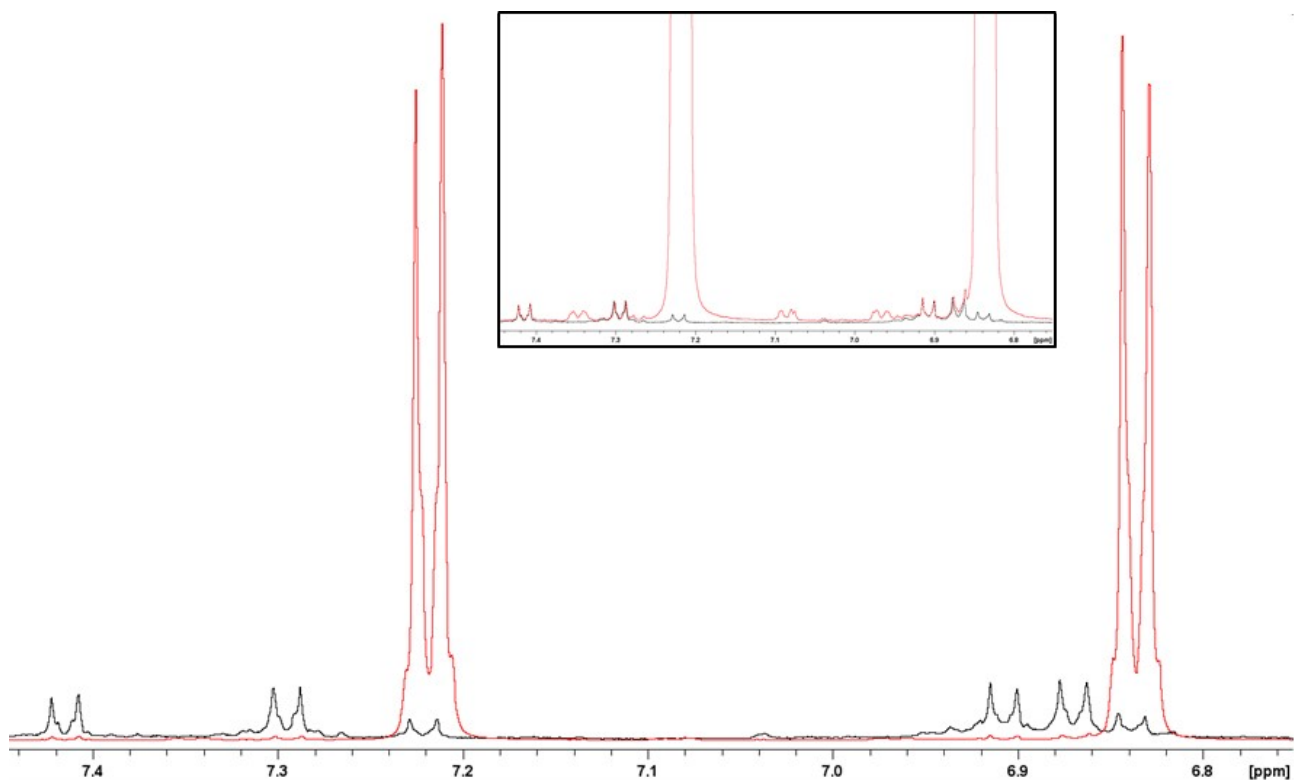


Figure S3. ¹D ¹H spectra (aromatic region) of the dispersant (in black) and of the dispersant after adding 2mM BPA (in red). The representative peaks of BPA increase in intensity and correspond to the peaks of the dispersant as shown by the arrows, confirming the presence of BPA. The intensity of red spectrum has been reduced of about 10 times to allow the complete observation of the peak. Inset: the same spectra with the real intensity. Other signals are aromatic compounds coming from the photo-degradation process.

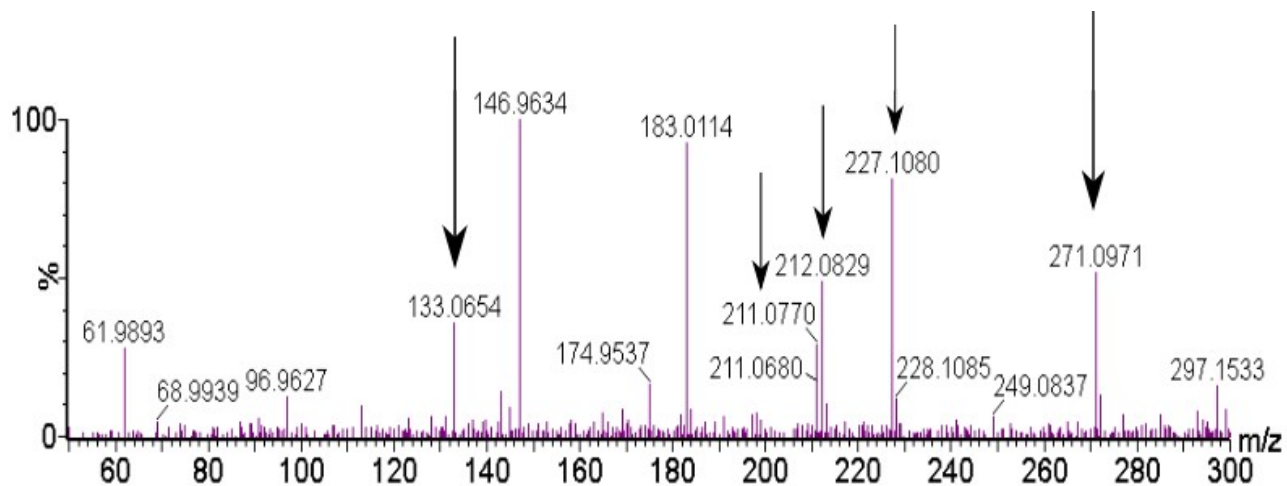


Figure S4. Corresponding MS/MS spectrum of one of the intermediates detected in the dispersant after the separation by the NPs population. The diagnostic MS/MS fragment ions, that confirm P271 structure for our unknown compound, are tagged by black arrows.

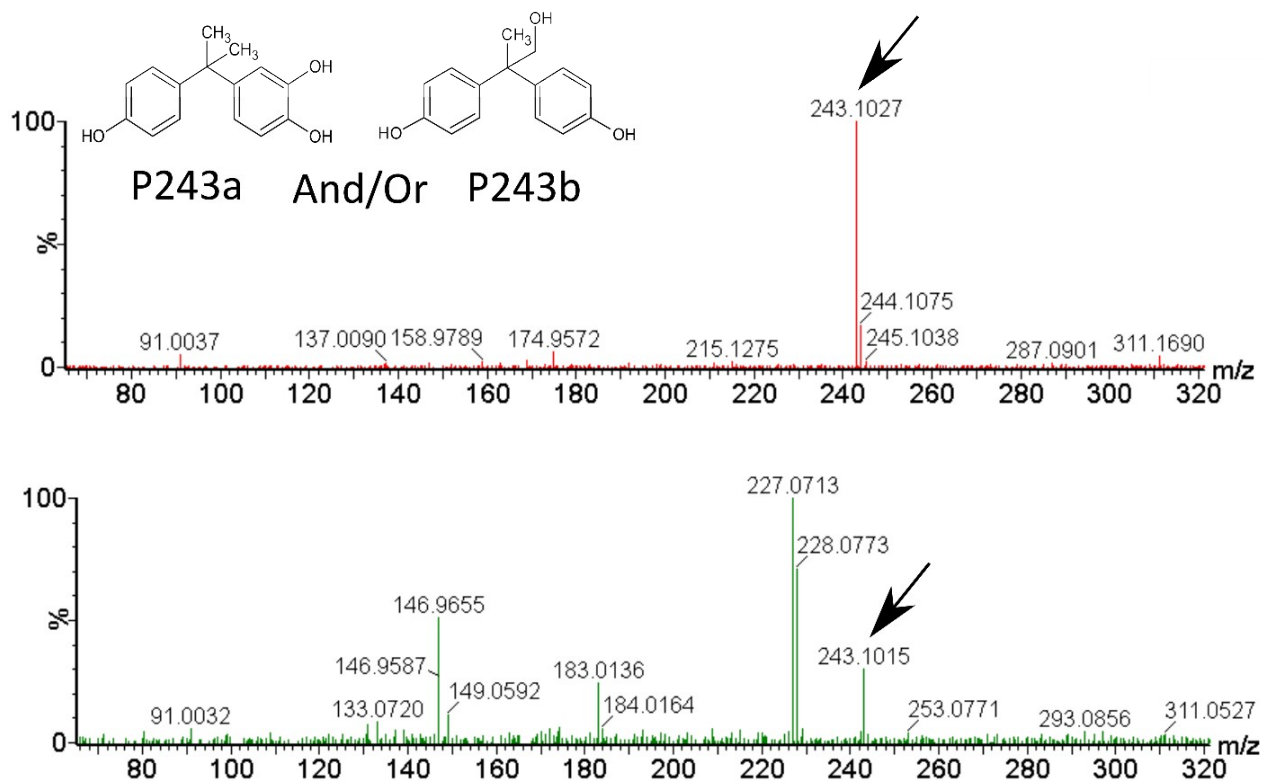


Figure S5. High-resolution MS/MS spectra of two isomeric species at 243.1 m/z, likely corresponding to degradation products P243a and P243b reported by Shi et al. 2021⁵.

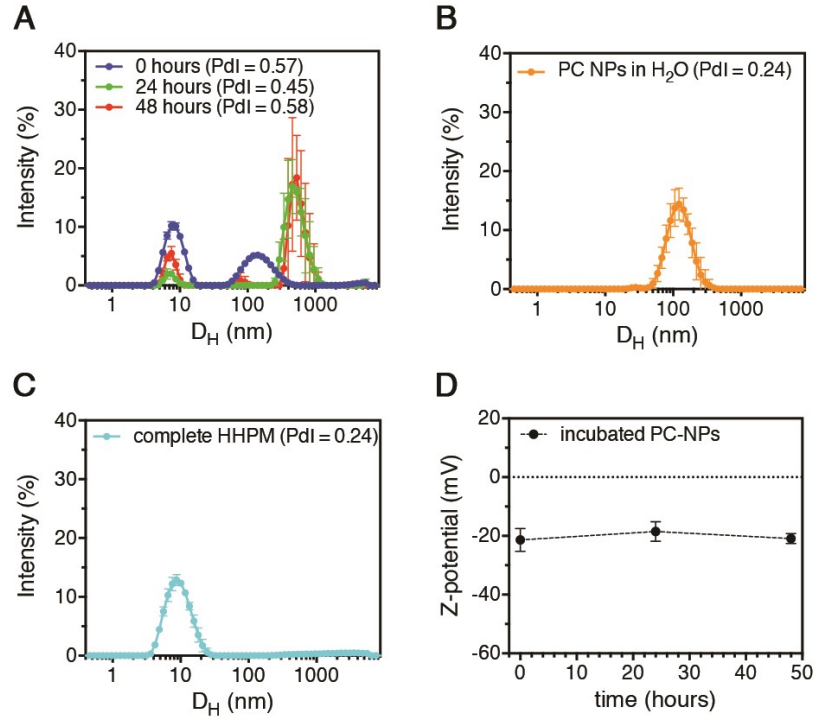


Figure S6. (A) Characterization of PC-NPs. Size distribution profiles obtained via DLS analysis relative to PC-NPs incubated in complete HHPM (final concentration: 30 $\mu\text{g/mL}$) for 0 (blue curve), 24 (green curve), or 48 hours (red curve). (B) Size distribution profiles of bare PC-NPs (*i.e.*, dispersed in Milli-Q[®] water; final concentration: 30 $\mu\text{g/mL}$) by DLS analysis. (C) Size distribution profiles of un-supplemented complete HHPM (*i.e.*, the fully supplemented culture medium used for UHs), by DLS analysis. (D) Surface charge of particle-corona complexes derived from the incubation of PC-NPs in complete HHPM for 0, 24, and 48 hours and isolated as reported by Maiorano et al. ¹, measured via Z-Pot analysis.

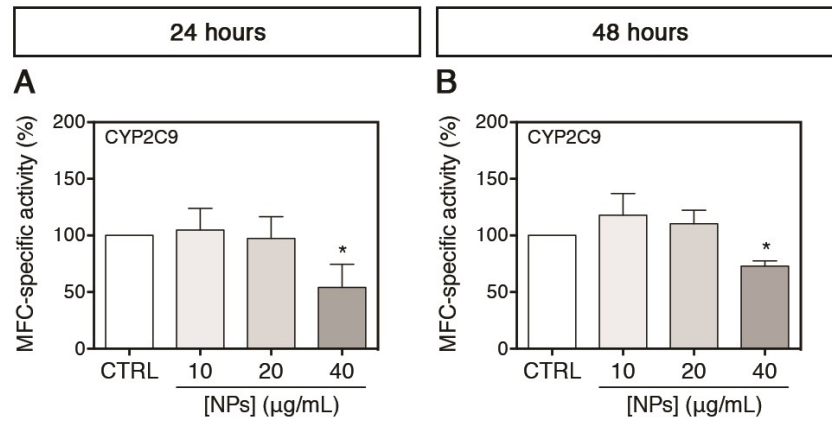


Figure S7. (A, B) MFC-specific metabolic activity of CYP2C9 in cells treated with PC-NPs or untreated (indicated as CTRL) for 24 (A) and 48 hours (B). Data are expressed as percentage values over CTRL (set as 100%). Results are reported as means \pm SD of three independent experiments. The symbol * refers to $p < 0.0500$, calculated *versus* CTRL for each treatment time (ordinary one-way ANOVA).

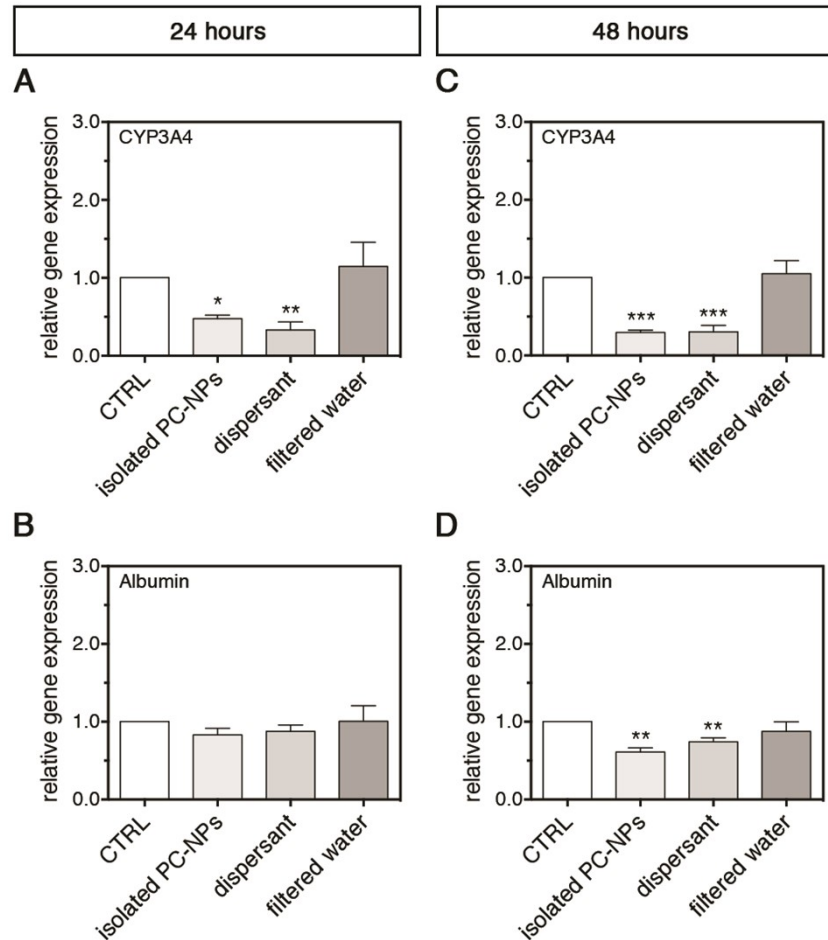


Figure S8. Effects of the two main components of the PC-NPs dispersion on the gene expression of CYP3A4 and Albumin. (A-D) Relative gene expression of CYP3A4 and albumin in cells treated with isolated PC-NPs or dispersant and un-treated (indicated as CTRL) for 24 (A, B) and 48 hours (C, D). “Filtered water” indicates the negative control, represented by cells treated with complete HHPM supplemented with ultra-filtered Milli-Q® water (for technical details, see Material and Methods). Results are means \pm SD of at least two independent experiments. The symbols *, **, and *** refer to $p < 0.0500$, $p < 0.0100$, and $p < 0.0005$, respectively, calculated *versus* CTRL for each treatment time (ordinary one-way ANOVA).

Supplementary Tables

Table S1. Assignment of the Raman modes of polycarbonate.

Wavenumber (cm ⁻¹)	Mode
407.1	O-C-O bend
537.8	Phenyl ring vibration
646.0	Phenyl ring vibration
721.9	C-H bend (out of plane (op))
829.7	Phenyl ring vibration
896.8	O-C(O)-O stretch
1118.8	O-C-O stretch
1189.8	O-C-O stretch
1245.9	O-C-O stretch
1462.3	CH ₃ symmetric bend
1611.9	Phenyl ring stretch
1787.6	C=O stretch
2880.6	C-H stretching
2978.1	C-H stretching
3078.3	C-H stretching

Table S2. Percentage of respective elemental composition of survey spectra.

	Binding Energy	PC pristine	PC NPs/C2F4
C 1s	284.7 eV	78.6%	34.7%
O 1s	532.2 eV	16.2%	53.0%
Si 2p	102.2 eV	5.2%	0.5%
Na 1s	1071.16 eV		11.8%

Table S3. Percentage of the areas of the deconvolution curves of the C1s spectra for the PC NPs, PC pristine films and PC ablated areas of the films. The C-F₂ signal is attributed to Teflon substrate.

C 1s	Binding Energy	PC pristine	PC NPs/C2F4
C-C, C-H (ar, al)	284.8 eV	83.4%	65.3%
C-O-C, C-OH	286.3 eV	8.7%	19.9%
C=O	287.7 eV	--	3.7%
O=C-O	288.7 eV	1.9%	8.9%
O=C(-O) ₂	290.4 eV	2.6%	2.2%
C-C sh.-up (I)	291.3 eV	2.2%	--
C-C sh.-up (II)	292.5 eV	1.2%	--

Table S4. Hydrodynamic diameter (D_H) mean values of the PC-NPs population, along with their relative intensities, in Milli-Q[®] water or complete HHPM (final concentration: 30 $\mu\text{g/mL}$), obtained via DLS analysis.

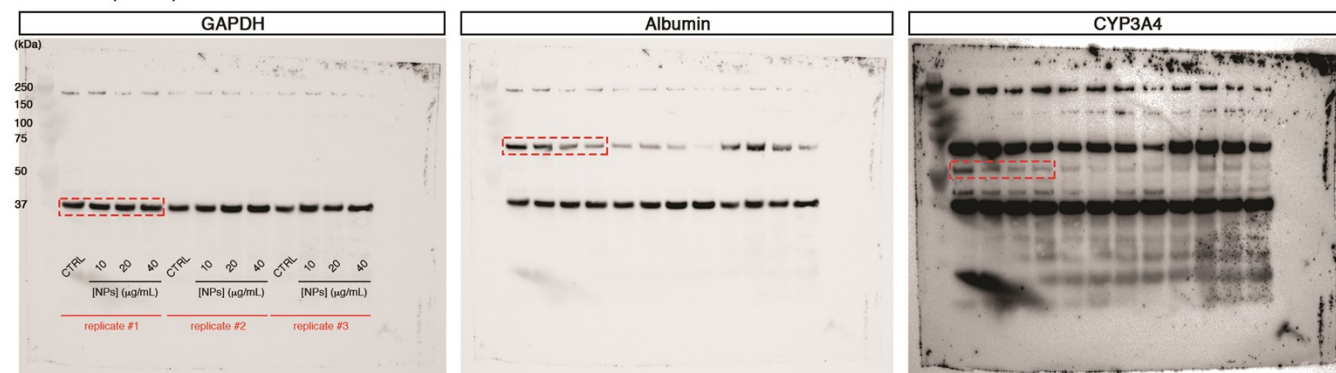
Dispersant	Incubation	Peak #1		Peak #2		Peak #3	
	Time (hours)	Size (d.nm)	Intensity (%)	Size (d.nm)	Intensity (%)	Size (d.nm)	Intensity (%)
Milli-Q [®] water	-	-	-	131.6 \pm 18.3	99.3		
complete HHPM	0	8.5 \pm 0.1	55.5	159.2 \pm 11.0	42.7	4476.0 \pm 248.9	1.7
	24	7.4 \pm 0.6	6.5	529.0 \pm 99.1	93.1	5560.0 (n = 1)	0.4
	48	7.3 \pm 0.3	17.4	569.0 \pm 125.0	80.1	-	-

Note. “n = 1” refers to the detection frequency of the corresponding peak in three consecutive measurements. The symbol ‘-’ means that peak has been not detected.

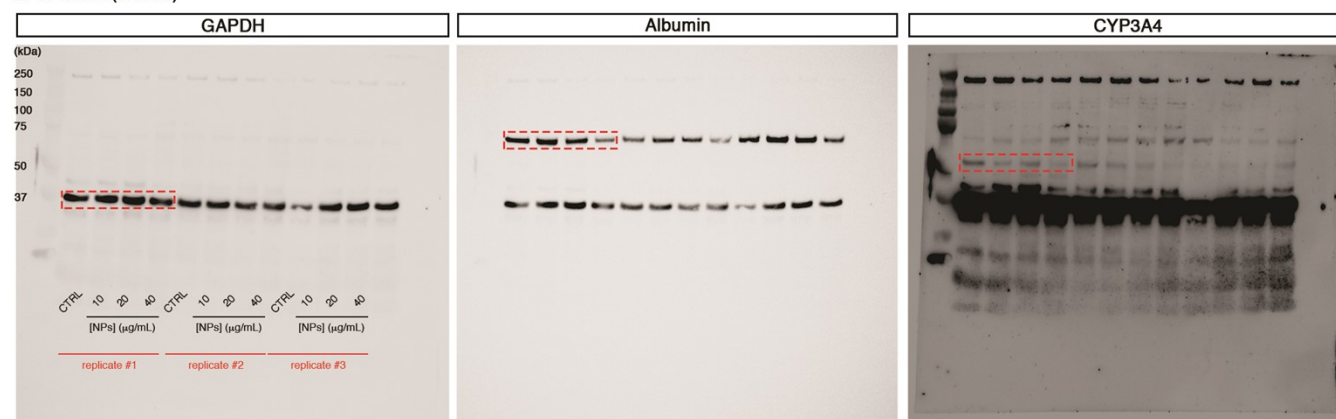
Raw Data

Western blot

A 24 hours (blot #1)



B 48 hours (blot #2)



Note. Original western blots relative to the total protein content from cells treated with PC-NPs or untreated (indicated as CTRL) for 24 (A) and 48 hours (B). For each time interval, samples from three biological replicates (replicate #1, replicate #2, replicate #3) were run simultaneously on the same gel, and the corresponding blot was probed consecutively with antibodies raised against CYP3A4, albumin, and GAPDH (for additional technical details, see section S9). Red selections indicate the boundaries whereby the lanes are cropped to be reported in the main text (Figure 7, panels A and C).

References

- 1 G. Maiorano, S. Sabella, B. Sorce, V. Brunetti, M. A. Malvindi, R. Cingolani and P. P. Pompa, Effects of Cell Culture Media on the Dynamic Formation of Protein–Nanoparticle Complexes and Influence on the Cellular Response, *ACS Nano*, 2010, **4**, 7481–7491.
- 2 D. Magrì, P. Sánchez-Moreno, G. Caputo, F. Gatto, M. Veronesi, G. Bardi, T. Catelani, D. Guarnieri, A. Athanassiou, P. P. Pompa and D. Fragouli, Laser Ablation as a Versatile Tool To Mimic Polyethylene Terephthalate Nanoplastic Pollutants: Characterization and Toxicology Assessment, *ACS Nano*, 2018, **12**, 7690–7700.
- 3 J. Bañuls-Ciscar, F. Fumagalli, A. Ruiz-Moreno, F. Rossi, S. V. Suraci, D. Fabiani and G. Ceccone, A methodology to investigate heterogeneous oxidation of thermally aged cross-linked polyethylene by ToF-SIMS, *Surf. Interface Anal.*, 2020, **52**, 1178–1184.
- 4 F. Bennet, A. Müller, J. Radnik, Y. Hachenberger, H. Jungnickel, P. Laux, A. Luch and J. Tentschert, Preparation of nanoparticles for ToF-SIMS and xps analysis, *J. Vis. Exp.*, 2020, **2020**, 1–26.
- 5 Y. Shi, P. Liu, X. Wu, H. Shi, H. Huang, H. Wang and S. Gao, Insight into chain scission and release profiles from photodegradation of polycarbonate microplastics, *Water Res.*, 2021, **195**, 116980.
- 6 P. Chomczynski, A reagent for the single-step simultaneous isolation of RNA, DNA and proteins from cell and tissue samples, *Biotechniques*, 1993, **15**, 532–537.
- 7 A. Romaldini, R. Spanò, F. Catalano, F. Villa, A. Poggi and S. Sabella, Sub-Lethal Concentrations of Graphene Oxide Trigger Acute-Phase Response and Impairment of Phase-I

Xenobiotic Metabolism in Upcyte® Hepatocytes, *Front. Bioeng. Biotechnol.*, ,

DOI:10.3389/fbioe.2022.867728.

- 8 M. W. Pfaffl, A new mathematical model for relative quantification in real-time RT-PCR, *Nucleic Acids Res.*, 2001, **29**, 45e – 45.